

THALES long wave QWIP thermal imagers

E. Costard *, Ph. Bois

THALES Research and Technology, RD 128, F-917674 PALAISEAU Cedex, France

Available online 22 November 2006

Abstract

THALES have developed for volume manufacture high performance low cost thermal imaging cameras based on the THALES Research Technology (TRT) third generation gallium arsenide long wave QWIP array. Catherine XP provides 768×575 CCIR video resolution and Catherine MP provides 1280×1024 SXGA video resolution. These compact and rugged cameras provide 24 h passive observation, detection, recognition, identification (DRI) in the $8\text{--}12 \mu\text{m}$ range, providing resistance to battlefield obscurants and solar dazzle, and are fully self contained with standard power and communication interfaces. The cameras have expansion capabilities to extend functionality (for example, automatic target detection) and have network battlefield capability. Both cameras benefit from the high quantum efficiency and freedom from low frequency noise of the TRT QWIP, allowing operation at 75 K, low integration times and non interruptive non uniformity correction. The cameras have successfully reached technology readiness level 6/7 and have commenced environmental qualification testing in order to complete the development programmes. These latest additions to the THALES Catherine family provide high performance thermal imaging at an affordable cost.

© 2006 Elsevier B.V. All rights reserved.

Keywords: QWIP; Infrared detectors; Focal plane arrays; Thermal camera

1. Introduction

In response to perceived future requirements and customer capability gaps, THALES identified in the early years of this decade a need to enhance its long wave IR camera product range which at that time was exclusively based on scanned long linear arrays of varying pixel count and pitch. An assessment of the candidate technologies indicated that uncooled microbolometers would in the timescale required provide insufficient performance and that cadmium mercury telluride LWIR arrays were still a number of years away from being viable. This left quantum well infrared photodetectors as the best technology to provide a route to high performance LWIR cameras.

Exploiting research on QWIP detectors carried out by THALES through the 1990s, a demonstrator camera based on a 384×288 $25 \mu\text{m}$ pitch QWIP detector was designed and built. This camera provided data that confirmed the

anticipated excellent temporal and spatial uniformity characteristics of gallium arsenide QWIP detectors as well as very high operability.

Following on from the demonstrator two programmes were launched to provide TV and SXGA resolution cameras, Catherine XP and Catherine MP. With a major focus on cost reduction it was recognised that by minimising the size of the array, costs could be kept low. However, by microscanning a small array to double the number of samples, the resolution could be recovered. Hence the approach of using standard 1/2 TV and full TV arrays to achieve the higher resolution outputs was adopted. This approach significantly reduced the costs of detector, the cooler, and the optics compared to the costs of similar components for use with larger arrays. Microscanning is made possible by the short integration time of the TRT QWIP.

2. Company background and programme definition

THALES Optroniques and THALES Optronics have been involved in the development of IR systems for over

* Corresponding author. Tel.: +33 169415768; fax: +33 169415738.
E-mail address: eric.costard@thalesgroup.com (E. Costard).

30 years. Their experience covers all application domains, including: tank fire control systems; submarine periscopes; ship defence systems; Infrared search and track for aircraft systems; and pilot night vision systems.

THALES Research and Technology (TRT) conducts research in many technology areas and, in particular, for the past 10 years, cooled gallium arsenide quantum well infra-red photoconductor (QWIP) arrays for night vision applications. This research has culminated in the production of practical high-resolution staring arrays in the LWIR (8–12 μm).

3. Background to the choice of the QWIP detector

Looking at the available technologies purely on a material basis, it appears that the vastly superior quantum efficiency of CMT ought to make this the obvious material to use. However, there are also limits set by silicon technology. Any large array needs to be used with a ROIC, and this ROIC will always have a limited well size. As the array pitch becomes smaller, the limitations on well size become more stringent. Integration times are normally chosen so that the wells are full (or approaching full) at the maximum required scene temperature. With a fixed well size, an increase in quantum efficiency immediately requires the use of a shorter integration time so as to avoid well overfilling. In simple terms, once the major parameters such as waveband have been chosen, the sensitivity depends principally on the well size, and not on the quantum efficiency. Provided the well can be filled in the time available (less than 7 ms for the two cameras in question), increasing the quantum efficiency does not improve the temperature sensitivity. This simple description covers only first order effects. The QWIP, when used at operating temperatures compatible with a compact camera, also has dark current that contributes to the well filling and degrades the available thermal sensitivity. For the cameras described, the integration time using QWIP technology is in the range 3–5 ms; using CMT it would be 20–50 μs . While the much longer integration time of the QWIP does give some image smear with moving targets, it should be noted that the 5 ms integration time mentioned above is shorter than the 12 ms response time of even a fast LCD display. For a camera to be used by a human observer, the QWIP is amply fast enough.

THALES has a long and successful history in non-uniformity correction of long linear CMT arrays. This experience led to the conclusion that more stable detectors would provide a route to cost reduction. The ability of a thermal camera to perform useful tasks is often dominated by the spatial noise, rather than the temporal noise. These two effects make roughly equal contributions to the performance when the spatial noise is 1/3 of the temporal noise – or, in other words, unless the spatial noise is reduced to less than 1/3 of the temporal noise, the performance will be dominated by that spatial noise. To achieve good field performance, the array uniformity has to be

corrected to and maintained below a few millikelvins, both over time and over the whole range of scene temperatures.

Interruptive non-uniformity correction is becoming unacceptable to users, and so either the array has to be good enough to remain stable to a few millikelvins over extended periods and extended temperature ranges (and no detector yet invented, not even a QWIP, does), or some scene-based correction must be used. Scene based methods are slow, as it is necessary to separate what is scene from what is non-uniformity, and this clearly cannot be done in a single frame. Scene-based methods therefore work only with detector arrays that drift slowly.

LWIR QWIPs meet this requirement of slow drift. Both the cameras described here use an initial factory calibration followed by a refinement of offset using scene-based methods.

THALES has chosen to use QWIP detectors for Catherine XP and MP because these detectors provide cameras with the characteristics desired by our customers. These characteristics are low cost, high definition and high quality images. QWIP detectors meet all these requirements. In the medium term, QWIP detectors currently provide the only available route to large format LWIR cameras. In the long term, it appears that the superior drift characteristics of QWIP arrays will always provide camera performance superior to that of other LWIR technologies. It also appears that military users will continue to prefer LWIR to MWIR, because of reduced effects of clutter and battlefield obscurants in the longer waveband.

4. Camera characteristics

Catherine XP (Fig. 1) and Catherine MP (Fig. 2) complement each other, providing solutions for different applications. Their general characteristics are compared in Table 1 below. Catherine MP has higher resolution than the Catherine XP but Catherine XP has smaller size and lower power consumption.

The cameras use common design approaches, with the main driver being to accommodate extensive functionality and good performance in very small packages. Both designs were cost-driven.



Fig. 1. Catherine XP in 4° version (left) and 3° version (right).



Fig. 2. Catherine MP camera.

5. TRT QWIP technology

For the last 5 years, the THALES Group has been manufacturing sensitive arrays using QWIP technology based on AsGa techniques through TRT Laboratory. End of 2005 TRT moved in new facilities with 250 m² class 1000/100 clean room now dedicated to the QWIP array production.

5.1. MBE growth

TRT proceeded in 2005 to a transfer from single to multi-wafer Riber 49 molecular beam epitaxy (MBE) system for the QWIP Epi-structures. With the Riber As/P Process Technology Center (PTC) we tested the reproducibility of the RIBER 49 system from run to run over 96 h. Effusion cells used for Ga and Al materials were left at

growth temperature all the time (i.e. 96 h). This time corresponds to the growth of a batch of 12 platens (5 × 3" each) of QWIP structures. Fig. 3 gives the absorption measurements on four substrates, chosen among the 96 h campaign: it highlights a wavelength variation of only ±0.17 μm, resulting in a perfect control of the growth rate.

5.2. QWIP array processing

THALES realizes the design and fabrication of the QWIP arrays, and the hybridization and integration in IDCCA are Sofradir's tasks. The QWIP processing is perfectly compatible with the Sofradir industrial procedures. The SEM photograph of Fig. 4 shows a detail of a classical 20 μm pitch array before hybridization. Systematic use of plasma etching makes possible very high filling factors (>85%) and a strict control of dimensions preserving the intrinsic epitaxial uniformity.

The fabrication yields obtained today on a GaAs wafer are above 70%, and the operating yield per array is better than 99.9% even for the full TV format (640 × 512) FPAs. Hybridization and GaAs substrate thinning are completely mastered by Sofradir. The SEM pictures of Fig. 5 show in cross section a 384 × 288 FPA before and after this thinning step. Figs. 6 and 7 report the main performances of the regular QWIP active layer used for the LWIR IDCCA products.

6. IDCCA performance estimation

In a end user point of view, a QWIP detector seems to be more complex than any other detector. Except the internal absorption all other intrinsic electro-optics parameters vary with the applied bias. The operating set point (bias voltage,

Table 1
Catherine camera characteristics

Camera	Catherine XP	Catherine MP
IDCCA	VEGA-LW (Sofradir)	SIRIUS-LW (Sofradir)
Detector	LWIR QWIP	LWIR QWIP
IDCA format	384 × 288	640 × 512
Array pitch	25 μm	20 μm
IDCA field rate	100 Hz	100 Hz
Microscan	2 × 2	2 × 2
Image format	768 × 575 (CCIR TV)	1280 × 1024 (SXGA) plus CCIR TV
Optical fields of view	9° × 7° and 3° × 2.25° (optional 10° × 7.5° and 4° × 3°)	15° × 12° and 5° × 4°
Ezoom	×2	×2, ×4 zoom (SXGA) × 1.67 (CCIR)
Operating temperature	>75 K	>73 K
Instantaneous IR scene dynamics (gain 1)	100 K	100 K
NETD	Measured as 55 mK	Measured as 55 mK
Non-uniformity correction method	Factory setting of gain and offset, plus scene-based update of offset	Factory setting of gain and offset, plus scene-based update of offset
Outputs	Analogue: CCIR TV Serial: digital 8 or 14 bit	Analogue: SXGA and CCIR TV Serial: digital 8 or 14 bit
Control	RS422 serial link or Canbus	RS422 serial link
Dimensions	258 × 172 × 100 mm	280 × 215 × 150 mm
Weight	3 kg	7.9 kg
Power consumption	30 W	34 W

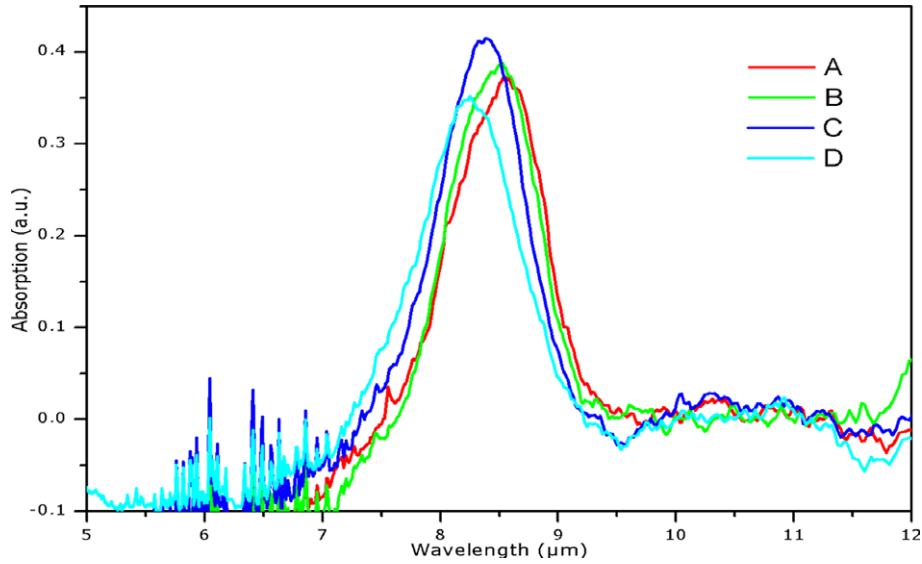


Fig. 3. Absorption spectra of 4 QWIP batches over 96 h.

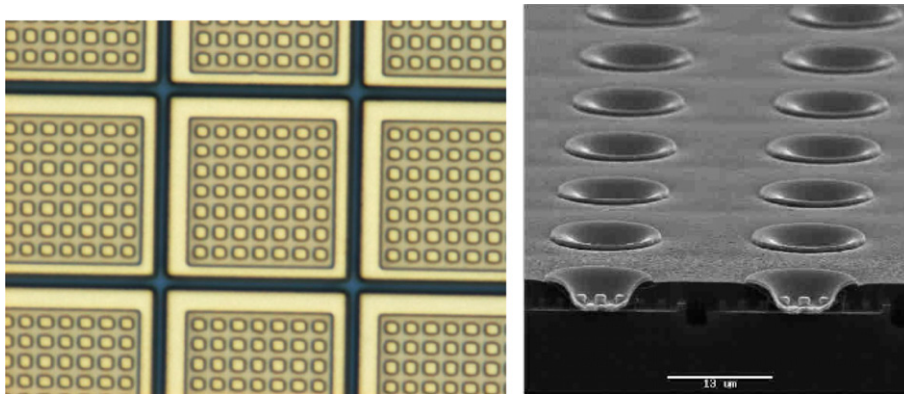


Fig. 4. Detail of a 384×288 classical QWIP array before hybridization.

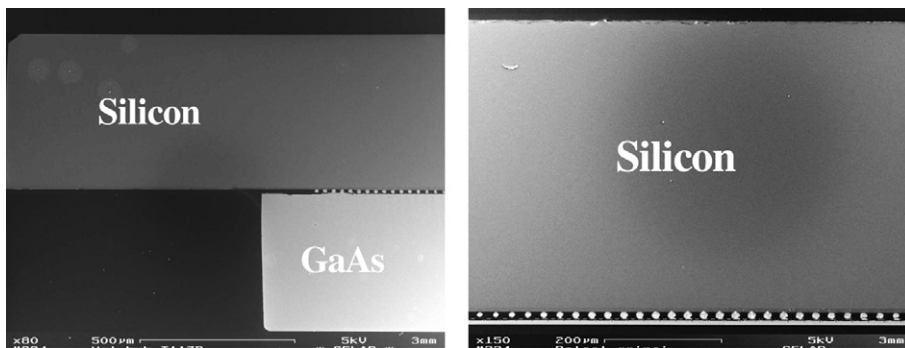


Fig. 5. SEM cross section before and after GaAs substrate removal.

integration time and operating temperature) has to be optimised for each application. This statement makes customers and some IR experts reluctant to consider QWIP. We developed a complete procedure in order to help the end user to set the thermal imager. We explain our approach hereafter.

The electro-optical characteristics of QWIPs are now well mastered and reliable models available. The dark cur-

rent is thermally activated and fully characterized by its activation energy (connected to the response peak wavelength) and an experimental $I(V)$ characteristic at liquid nitrogen temperature. The noise is mainly due to generation–recombination processes and can be described by a simple photoconductive model, introducing the noise gain. No low frequency noise is observed in QWIPs. The

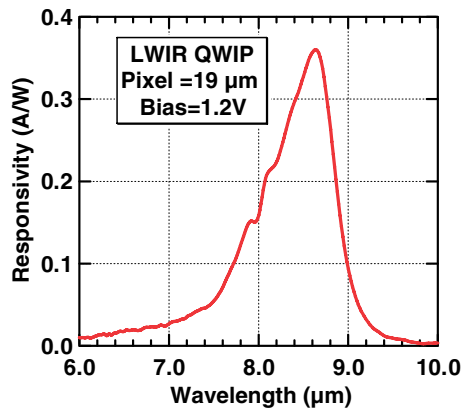


Fig. 6. Typical spectral response of LW QWIP IDDCA (before thinning and AR coating).

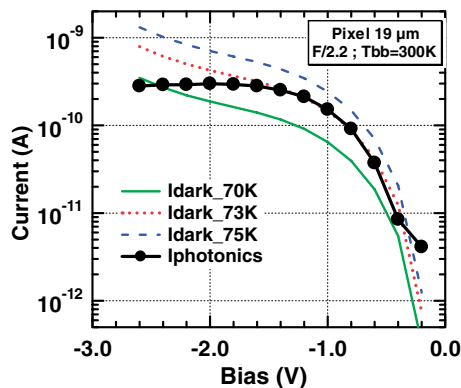


Fig. 7. Typical dark current of LW QWIP IDDCA.

absorption is quite insensitive to the applied bias, as well as to the detector temperature. So, the responsivity can be described by a unique, bias independent spectral shape and by the peak responsivity curve versus applied bias.

Yet, one should not forget that the responsivity strongly depends on the optical coupling scheme (e.g. 2D diffraction gratings) and on the pixel size [1]. So, in order to obtain pertinent values, the measurements must be performed on pixels identical to those composing the real FPAs. Different configurations (e.g. 45° facet coupling or large pixels) cannot be exploited to assess the final IDDCA performance. These points are illustrated below. Fig. 8 shows the normalised spectral shape for large (150 μm) pixels without and with diffraction gratings. The former configuration is similar to the 45° facet coupling.

The use of a diffraction grating, or any other resonant coupling schemes, strongly affects the spectral shape and also the peak amplitude, due to the intrinsic resonant coupling efficiency. This clearly demonstrates that 45° facet measurements, as well as grating-less pixel measurements cannot be retained as reliable data for FPA performance assessment.

Fig. 9 illustrates the evolution of the responsivity with the pixel size. Decreasing the pixel size from 150 μm down to 20 μm causes the response peak to become wider and the

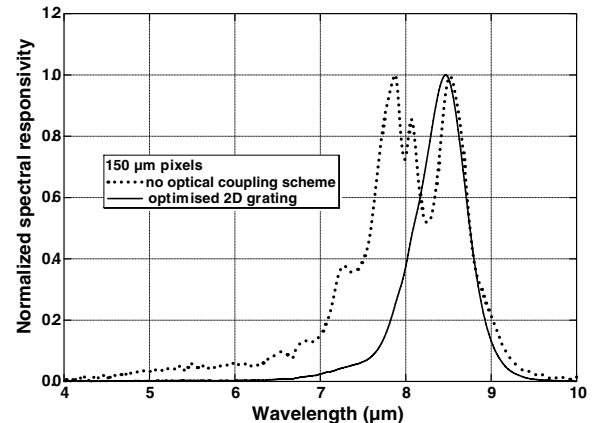


Fig. 8. Spectral shape with and without optical coupling scheme.

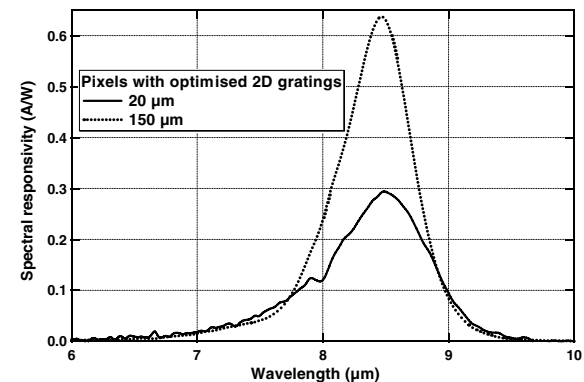


Fig. 9. Influence of the pixel size on the responsivity.

peak amplitude to shrink by as much as 50%. Consequently, experimental measurements have to be performed on pixel configurations identical to those used for FPAs. This is the case for all the samples presented in the following sections.

The detector characteristics (dark current, responsivity, noise gain) are used together with the ROIC characteristics (well capacity, output range, output noise), to calculate the IDDCA performance, according to the following procedure. First the maximum integration time is calculated, taking into account the mean scene temperature, instantaneous dynamic range and field of view. Next, IDDCA parameters (response (mV/K), noise (μV), NETD (mK)) are estimated. Calculations at fixed integration time or fixed well filling fraction are also possible. The transmission of the optics as well as extra noise sources can also be considered. Calculations apply to a pixel at the centre of the matrix, receiving the maximum IR flux. This procedure is used to set the best bias and integration time at a given operating temperature for a dedicated application.

We present now the performance estimations for a regular 9 μm QWIP structure designed at TRT and integrated in the SOFRADIR VEGA-LW IDDCA (388 × 284, 25 μm pitch, pixel size 23 μm) [2–5].

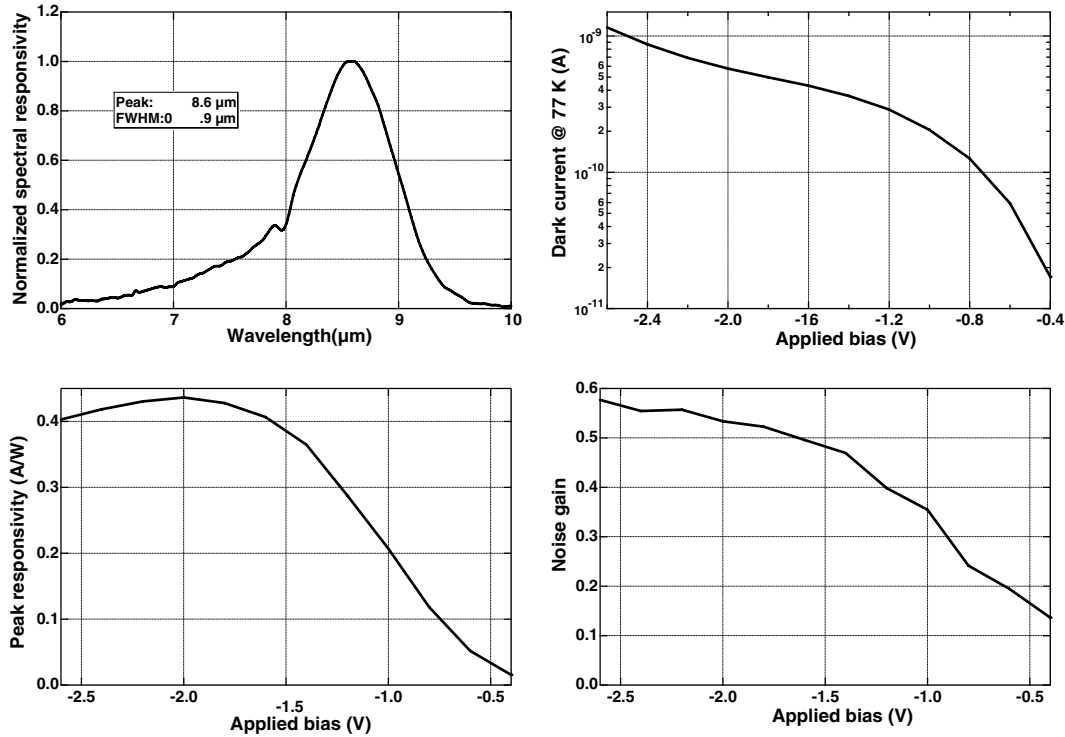


Fig. 10. Regular QWIP @ 9 μm : EO characteristics @ 77 K.

Fig. 10 presents the detector characteristics. The responsivity peaks at 8.6 μm (FWHM = 0.9 μm). At 1 V and 77 K, we measure a dark current of 0.2 nA and a peak responsivity of 0.2 A/W (with optimised anti-reflection coating).

For performance estimation the Indigo ISC0208 ROIC is once again considered. Calculations are performed for a 293 K mean scene temperature, $F/2.7$ field of view (diffraction limited optics) and +50 °C instantaneous dynamic range (i.e. the integration time is chosen to get saturation in front of a blackbody set at 343 K). A 100 Hz frame rate, combined to micro-scan considerations, imposes the maximum integration time to be 5 ms.

The resulting performances are presented in Fig. 11, as a function of temperature and applied bias. These curves allow the determination of the optimum bias for each temperature. In the case presented here the ultimate performance is limited by the maximum integration time.

The calculated data at 75 K and 1.2 V (response = 12.5 mV/K, NETD = 40 mK, $T_{\text{int}} = 5$ ms) are in good agreement with experimental parameters measured at Sofradir on operational IDDCAs (75 K, response = 12.3 mV/K, NETD = 54 mK, $T_{\text{int}} = 4$ ms), and especially with the 49 mK measured in the same conditions and with the same IDCCA integrated in a Catherine-XP Thermal imager [5].

7. Operating temperature considerations

We will make use of the SIRIUS-LW IDCCA from Sofradir to illustrate the influence of the operating temperature on FPA performances.

7.1. SIRIUS-LW: ROIC and dewar description

In order to obtain a technical breakthrough with the competition offering large arrays (640 \times 512 at 25 μm pitch) working at low temperature (≤ 65 K) with heavy split stirring coolers, the maximum compactness was required for this new SIRIUS-LW detector (Fig. 12). A frame rate above 100 Hz was also required to offer a SXGA high definition image (1280 \times 1024) at standard 25 Hz or 30 Hz video frame rate at camera level when using a microscanning system. SIRIUS-LW can therefore equip third generation LW FLIRs to compete with the high resolution second generation FLIRs using long scanned time and delay integration (TDI) arrays.

The ROIC pitch of 20 μm was chosen for cost and yield optimization, and for enabling the smallest dewar diameter. The integration while read mode was required for enabling the 120 Hz frame rate. Therefore, a new readout circuit was specifically designed for this format because commercially off the shelf ROICs were not offering these features.

The ROIC was previously described [6]. It was specifically developed for P/N QWIP structure, and offers a skimming mode for dynamic range optimization (suppression at sample/hold output level of the QWIP dark current from the dynamic range). It includes standard features for sofradir ROICs: direct injection; snapshot; IWR; 1/2/4 outputs, four gains ($\times 1$, $\times 1.3$, $\times 2$, $\times 4$); 10.3 Million electrons well fill for gain $\times 1$; Up to 10 MHz per output for 120Hz frame rate; 3.2 V dynamic range; image invert/revert/inverse; random windowing.

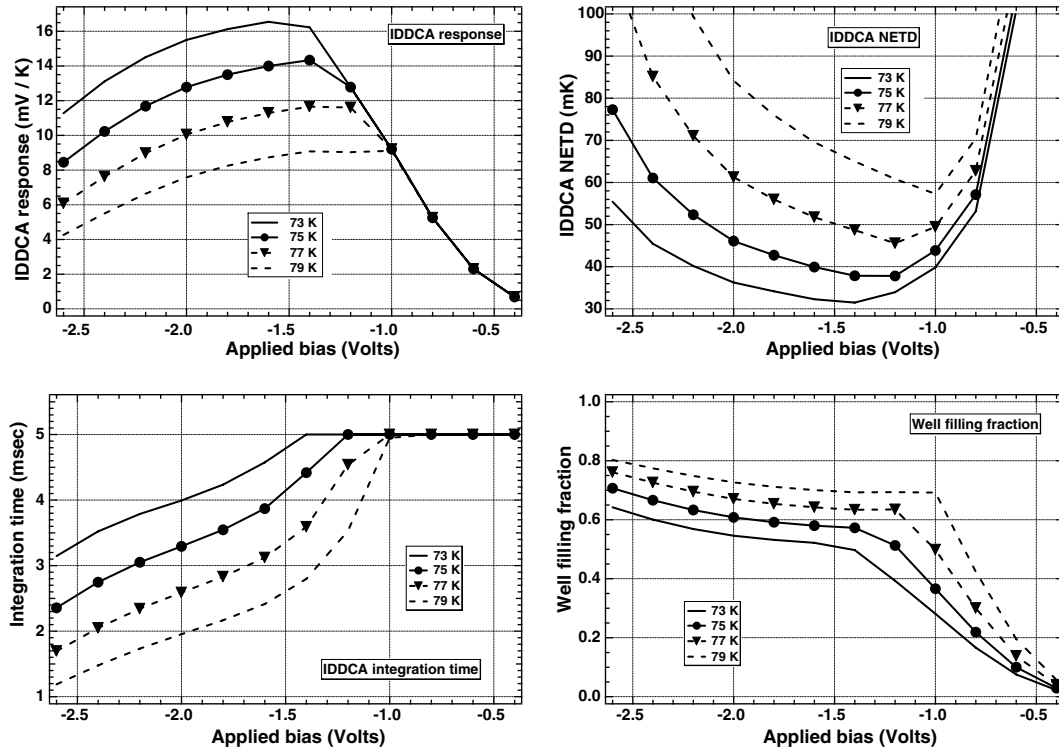


Fig. 11. Regular QWIP @ 9 μm: IDDCA estimated performance.

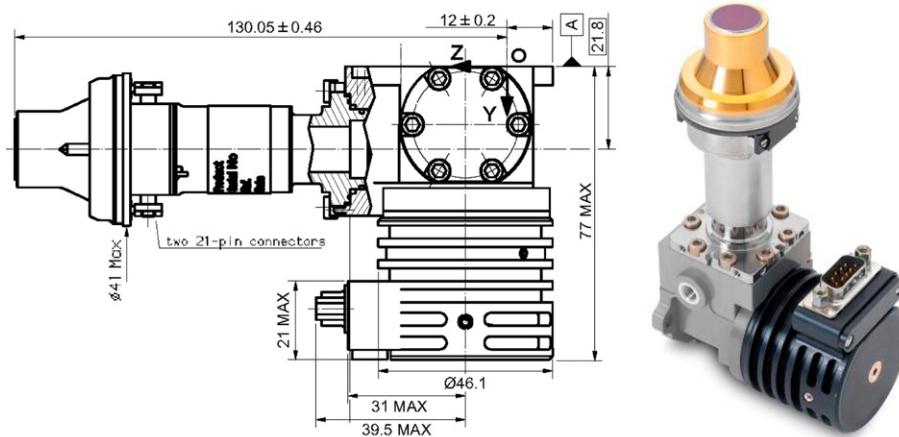


Fig. 12. 640 × 542 QWIP IDDCA with the “0.75 W class” K548.

A dewar was adapted to the Ricor (Israel) “0.75 W class” K548 rotary microcooler, for an operating temperature between 70 K and 75 K. The 9 mm diameter “large” cold finger of the K548 gives the IDDCA a high cryogenic power enabling very low cool down times and low regulated power, for >70 K operating temperature under any military ambient temperature conditions (up to 71 °C).

The 1.6 mm Germanium dewar window has a broadband anti reflection coating optimized for LW transmission (the QWIP detector itself is defining the spectral response). The cold shield has a 20 mm height (above the IRFPA), with an aperture up to 9 mm for $f/2.2$ applications. Smaller

aperture can be offered without dewar redesign. Larger aperture can be offered with top dewar redesign (cold shield, window and window cover). The IRFPA is integrated in a 40 mm diameter encapsulation (at IRFPA level). The dimensions are 142 mm height and 77 mm width. The total IDDCA weight is 0.65 kg (1.43 lb). The electrical interface is ensured thanks to two 21-pin connectors located below the Ø40 mm feedthru ceramics.

Specific care has been taken to integrate the IRFPA and the cold plate in order to minimize the thermal cycling constraints and therefore to maximize the IRFPA reliability by ensuring several thousands of thermal cycles (ONs/OFFs

of cooler) before any apparition of new defects in the array.

This IDDCA has been developed for military FLIRs conditions and is hardened against low resonance frequencies to sustain classical ground mobile (GM) environments with random vibrations spectrum up to 2000 Hz, as well as ambient temperatures up to 71 °C (IDDCA skin temperature).

7.2. SIRIUS-LW: E&O performance

The spectral response of the SIRIUS-LW detector is given in Fig. 6.

The measurement conditions or the customer system constraints in terms of frame rate (and therefore integration time), dynamic range or weight/power budgets (and therefore operating temperature) lead to different possible electro-optical performance.

The integration time is tuned at a value that ensures that the ROIC will not saturate in front of a 70 °C blackbody. The instantaneous dynamic range is therefore guaranteed to be +50 °C above ambient without any change of the settings (integration time or skimming or gain). This is an important point if comparison is made with other measurements presenting extreme performance but with a very low dynamic range (preventing such detector to be used in operation).

Seventy-three Kelvin is a working point that gives a satisfying tradeoff between NETD/detection range, and power consumption. At this temperature, one detector shows the following performance: for a $f/2.2$ aperture, in gain 1 (10.3Me⁻) in front of a 20 °C blackbody, and with $T_i = 4$ ms, the average 20–35 °C sensitivity is 23 mV/K and its standard deviation is 8.51% without field of view correction (Fig. 13). The average NETD is 41.4 mK and its standard deviation is 10.96% (Fig. 14). The typical operability (NETD > 2 × NETD_{average}) is 99.9% with no cluster of size >3 (Fig. 15).

Figs. 16 and 17 show the evolution of the sensitivity and of the NETD of this SIRIUS-LW IDDCA, when the FPA temperature changes from 65 K to 75 K. For each FPA

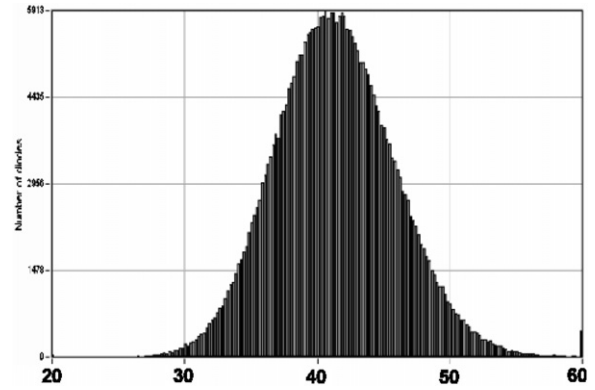


Fig. 14. NETD at 73 K (mK) (with FOV correction).

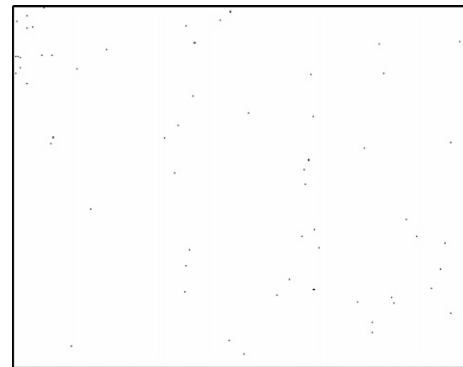


Fig. 15. Operability (NETD > 2 × mean).

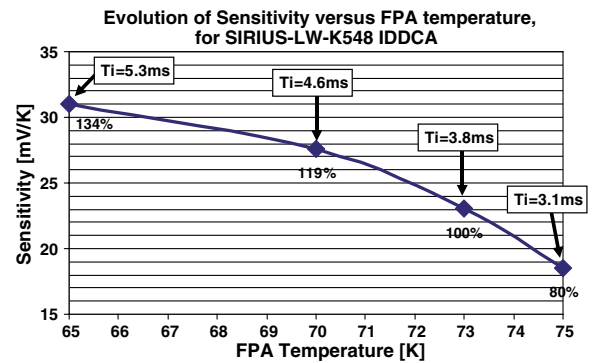


Fig. 16. Average sensitivity.

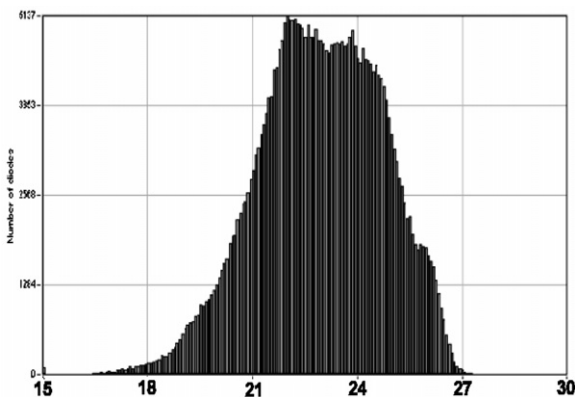


Fig. 13. 20–35 °C Sensitivity at 73 K in mV/K, no FOV correction.

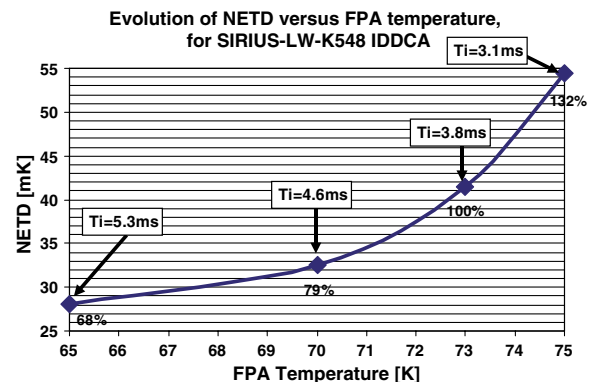


Fig. 17. Average NETD.

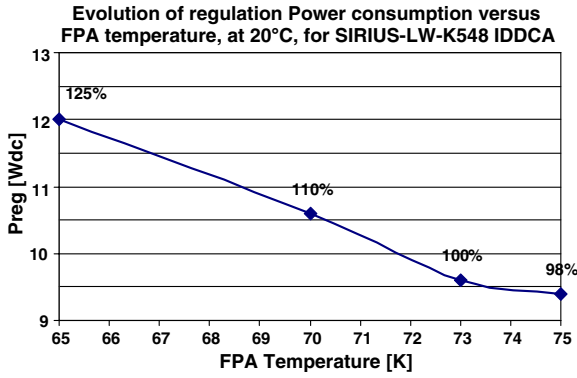


Fig. 18. Cooler power in regulation.

temperature, the integration time has been adjusted between 5.3 ms and 3.1 ms in order to comply with the instantaneous +50 K dynamic range requirement. The percentage values are the ratios with the performance at 73 K. There is a 20% performance increase when tuning the FPA at 70 K instead of 73 K. Of course, performance can still be improved if the instantaneous +50 K dynamic range requirement is reduced, thus enabling to increase the integration time accordingly.

7.3. SIRIUS-LW: Cryogenic performance

The compactness of the dewar, its high efficiency (minimized thermal mass and heat load), associated with the high cryogenic power of the K548 microcooler, enable SIRIUS-LW-K548 IDDCA to highlight impressive cryogenic performance:

Fig. 18 shows the evolution of the K548 cooler cryogenic power in regulation at 20 °C ambient, when the FPA temperature swings from 65 K to 75 K. The IDDCA regulates with 9.6 W_{DC} at 73 K, with 10.6 W_{DC} (+10%) at 70 K, and with 12 W_{DC} (+25%) at 65 K.

Depending on the expected electrooptical performance, the tradeoff with power consumption will be chosen.

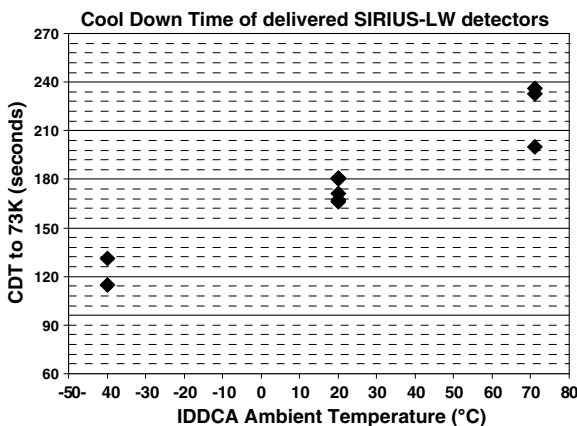


Fig. 19. Cool down time to 73 K for three IDDCA.

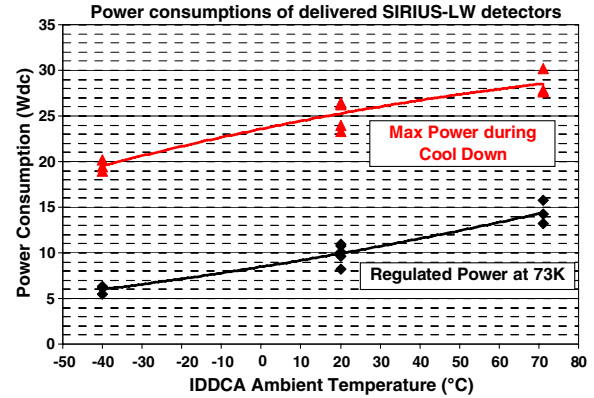


Fig. 20. Power consumption for three IDDCA.

Fig. 19 gives the Cool down time to 73 K of three IDDCA measured in climatic conditions. The CDT is <2.5 min at -40 °C, <3 min at +20 °C and <4 min at +71 °C. Fig. 20 gives the power consumption during cool down and regulation at 73 K of the same IDDCA: at 71 °C, the maximum power is less than 31 W_{DC} and the regulated power is less than 16 W_{DC}.

These power consumptions can be compared to other QWIP detectors working at 60 K or 65 K, for which the heavy split stirling engines exhibit power consumption in the range of 60–80 W during cool down and 25–40 W in regulation. The power saving is a direct benefit for the power budget of the FLIR as well as for the heat sink design.

8. Conclusion

Improvement of QWIP operating temperature introduces greater flexibility for the dewar and cryogenic cooling system. The newly accessible performances reduce (even cancel) the traditional operating temperature handicap of the QWIP GaAs detectors, while preserving the exceptional qualities of their electro-optical performances and other large focal plane industrial feasibility aspects.

This paper has presented two sophisticated LWIR cameras. Both exploit the unique characteristics of the TRT QWIP detector and also Sofradir’s skills for compact IDCA to provide affordable large-format LWIR imaging for their respective applications. The Catherine XP and Catherine MP cameras provide low cost, high quality, compact, thermal imaging capability for a wide range of applications. The capabilities of these cameras are, by virtue of their use of FPGAs, capable of extension to incorporate many features which would previously have been impossible inside a thermal camera.

Acknowledgements

The authors would like to thank the Sofradir teams of the Technical Department that managed to develop these challenging new IDCA products, and the camera integra-

tion teams of THALES for their efforts being rewarded today with thermal imagers successfully entering production.

References

- [1] A. De Rossi et al., *Infrared Physics and Technology* 44 (2003) 325–330.
- [2] A. Manissadjian, *OPTRO 2002*, Paris, January 14–16, 2002.
- [3] Les caméras thermiques portables, F.H. Gauthier, THALES Optronique, *OPTRO 2002*, Paris, January 14–16, 2002.
- [4] A. Manissadjian et al., *New Compact Staring Detectors for MW and LW Applications*, SPIE, Orlando, 2005 (5612-05).
- [5] W. Johnston et al., *THALES Long Wave Advanced IR QWIP Cameras*, SPIE, Orlando, 2006 (6206-17).
- [6] S. Crawford et al., *Beyond third generation MCT: SXGA QWIP*, in: *Proc. SPIE*, vol. 5783 pp. 777–788.